JOURNAL OF MATERIALS SCIENCE 40 (2005) 6553–6558

Oxidation behavior of *in situ* synthesized TiB/Ti-Al composite

YEXIA QIN, DI ZHANG, WEIJIE LU, JINING QIN, DONG XU
State Key Laboratory of Metal Matrix Composites, Shanghai JiaoTong University, Shanghai, 200030, People's Republic of China
E-mail: suzieq@sohu.com

Published online: 25 October 2005

The oxidation behavior of an *in situ* synthesized TiB reinforced Ti-Al-8(vol%)B composites (TMCs) and Ti-Al were studied at 823, 873, and 923 K in atmospheric air. The oxidation kinetics follows a parabolic rate law. The oxidation rate decreases gradually as the oxidation proceeds. Scanning electron microscopy (SEM) with energy dispersive X-ray spectrometry, and transmission electron microscopy (TEM) were used to identify oxidation products and characterize oxide scale morphology. The oxide scale formed on TMCs was predominantly rutile TiO_2 and α-Al_2O_3. No B_2O_3 and other oxides were observed within the oxide scale. The *in situ* synthesized TiB particles can increase the oxidation resistance of TMCs. It is attributed to the enhanced alumina-forming tendency, the formation of thin and dense oxidation, and the interface cohesion and the clean interfacial microstructure before and after oxidation between the reinforcements and the titanium matrix alloy.

1. Introduction

Structural materials used in high temperature applications, e.g., turbine blades for aircraft engines, should have good mechanical properties, e.g., strength and creep-resistance, at the operating temperatures. Particulate-reinforced titanium matrix composites (TMCs) can satisfy these conditions to a high degree. Those materials have a relatively low mass density of approximately 4×10^3 kg/m^3. The introduction of particulates with low density and high modulus into titanium alloys has significantly improved the specific modulus, specific strength, creep resistance, wear resistance and the service temperatures [1, 2]. Lu *et al.* [3, 4] have developed a new technology to manufacture the TiB-reinforced titanium matrix composites via a cost-effective *in situ* reaction process including traditional ingot metallurgy and self-propagation high-temperature synthesis (SHS). The TiB play a role in the formation of fine grains, and advantageously do not react with the matrix, thereby avoiding the formation of brittle reaction products at the reinforcement-matrix interface [5]. The *in situ* technology is becoming a promising industrial method to produce particulate reinforced titanium matrix composites in a large scale [6].

In addition to good mechanical properties, materials should possess good oxidation resistance at high temperature in order to expand the application. Therefore, the high temperature oxidation behavior of TMCs is of particular interest. However, it has been well known that the oxidation resistance of TMCs would not be sufficient at temperatures above 773 K in air. Until now little work has been carried out on the oxidation properties of TMCs, which is another important factor for use at high temperature [7].

The present study was undertaken to investigate the oxidation kinetics and mechanism of TiB particle-reinforced TMCs, which was fabricated by a SHS at temperatures of 823, 873, and 923 K in air. Characterization of the oxidation products, the structure and morphology of the oxide scale, and the metal subsurface layer was conducted.

2. Experimental procedures

On the basis of a previous paper [3], TMCs reinforced with TiB were fabricated by consumable vacuum arc remelting. Cast titanium metal matrix composites (TMCs) were used as the bulk alloy. The reagents used were grade two sponge titanium (99%), boron powder (90 pct, average particle size: 5 to 7 μm). The volume percentage of the reinforcement phase is 8%. The compositions of the raw material and the volume percentage of the reinforcements are listed in Table I.

The specimens with dimensions of $10 \times 10 \times 3$ mm were prepared using electric-wire cutting, polished on series of SiC polishing paper. After fabrication, the samples were first cleaned in acetone, then chemically etched in a solution of 4.2%HF + 12.5%HNO_3 + 83.3% H_2O for 60 s, and then rinsed in isopropyl alcohol in order to remove any residual enchant. The specimens were then dried in air, and weighed before

0022-2461
DOI: 10.1007/s10853-005-1688-2

TABLE I Compositions and reinforcements volume percentage in TiB/Ti-Al composites

Sample no.	Matrix alloy	Al (wt%)	B (wt%)	Reinforcements (TiB) (vol%)
TMCs	Ti	6.72	1.38	8.00
Ti-Al	Ti	6.72	0	0

oxidation. Their dimensions measured to an accuracy of 0.1 mm.

Oxidation tests on the prepared specimens were carried out isothermally in static air at 823, 873, and 923 K in order to obtain information about the oxidation kinetics of the TMCs. The total duration of the oxidation tests was 300 h. The oxidation data were then presented as the weight gain per unit area of exposed specimen vs time to describe the type of oxidation. The oxidation activation energy was then calculated from the oxidation data.

The surface of the oxidized specimen was examined. Scanning electron microscopy (SEM), X-ray diffraction (XRD) and X-ray photoelectron spectroscopy (XPS) techniques were employed to understand the nature and composition of the oxide scale formed during exposure to elevated temperatures.

The cross-section microstructure details of the composites after oxidation were carried out using a H-800 (200 kv) transmission electron microscope (TEM) and an EDAX energy dispersive X-ray (EDX) analysis system with windowless detector were available. Samples for TEM were prepared by the focus iron beam (FIB) thinning.

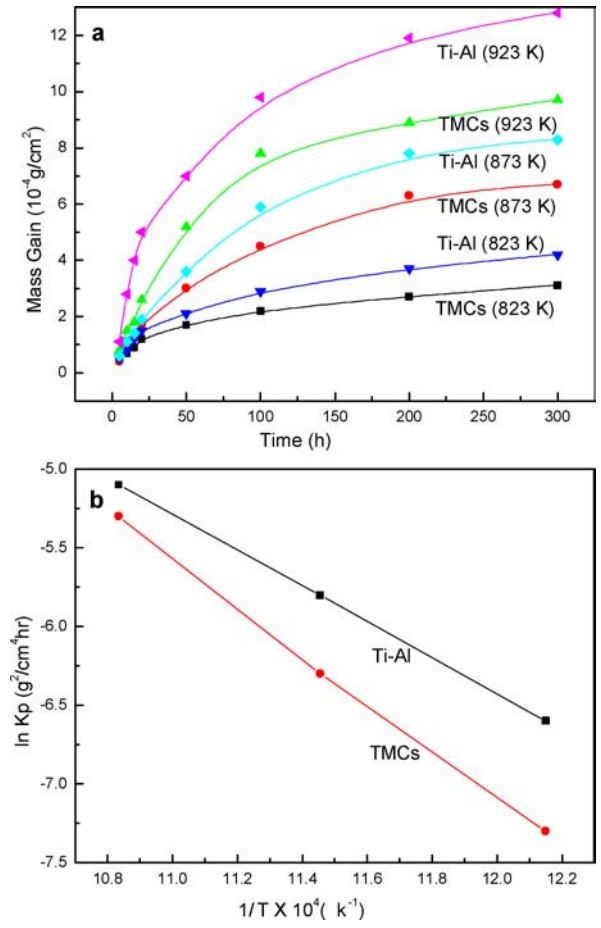

Figure 1 Oxidation kinetics for (a) TMCs, Ti-Al after oxidation at 823, 873, and 923 K for 300 h; (b) K_p versus 1/T for TMCs and Ti-Al.

TABLE II Activation energy for oxidation and diffusion in various titanium alloys [12]

Alloy stoichiometry (wt%)	Activation energy (KJ/mol)
Pure Ti	239
Ti-1.5wt%Al	183
Ti-9.7wt%Al	209
Ti-6.72wt%Al (present work)	225.8
Ti-15.81wt%Al	269
Ti-16.52wt%Al	255
Ti-22.5wt%Al	299
Ti-8.5Al-1B-1Si	303
Ti-6Al-8vol%TiB(present work)	297.6
O diffusion in TiO_2	234
Ti diffusion in TiO_2	257
O fast diffusion paths in Al_2O_3	241
Al diffusion in polycrystalline Al_2O_3	477

3. Results and discussion

3.1. Oxidation kinetics

The respective kinetics of isothermal oxidation (in terms of mass gain per unit area as a function of time) for TMCs at 823, 873, and 923 K are presented in Fig. 1. As expected, the oxidation rates of all specimens tested increased with an increase in oxidation temperature. All specimens show almost the same oxidation trend. However, the rates of oxidation are found to be higher in Ti-Al than that for the TMCs at all temperatures. It is clear that the mass gains for the TMCs decrease when compared with Ti-

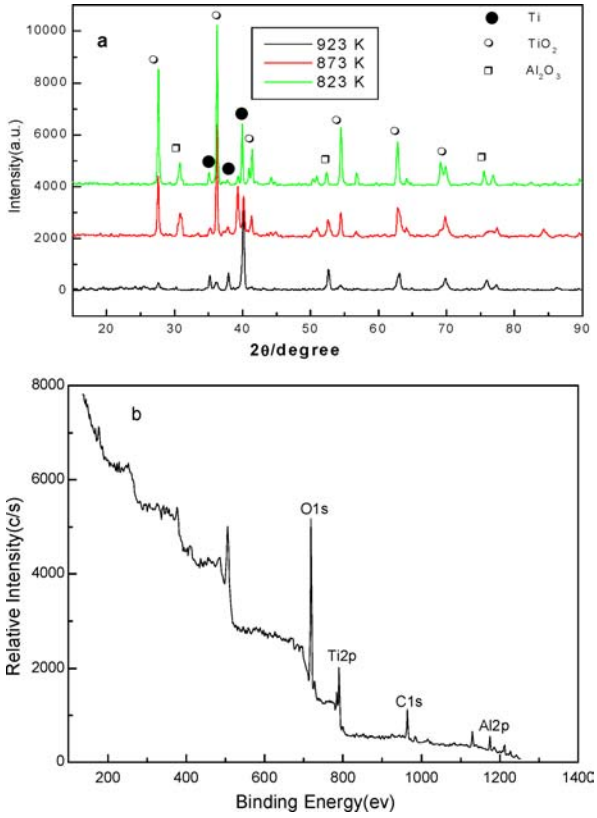

Figure 2 (a) Diffraction patterns of TMCs after oxidation at 823, 873, and 923 K, (b) XPS spectra of TMCs after oxidation at 873 K for 300 h.

Al indicating that the reinforcements can improve the resistance.

In general, the isothermal-oxidation kinetics expresses by a power law as:

$$(q)^n = K_p t \tag{1}$$

where, q, t, n, and K_p are the mass gain per unit area, time, reaction index, and rate constant, respectively [8]. The values of n were obtained from the reciprocal of the gradient of the logarithmic plot of q versus t for a given set of reaction. It is apparent that the oxidation kinetics follows parabolic (n=2) rate equation at all tested temperature for both the specimens. In certain cases the value of n is a constant at different temperatures of testing, and under those conditions, K_p follows an Arrhenius relation of the form

$$K_p = K_0 \exp(-Q_{\text{exp}}/RT) \tag{2}$$

where Q_{exp} = effective activation energy for oxidation, K_0 = constant for a given material, T the absolute temperature and R the universal gas constant.

Fig. 1b is plots of K_p versus $1/T$; the slopes of the plots yield the activation energy of oxidation of TMCs and Ti-Al, respectively. Table II also lists the activation energies for oxidation in the current tests as well as for various other systems. The activation energy for oxidation of TMCs is 297.6 KJ/mol and that of Ti-Al is 225.8 KJ/mol.

3.2. Metallography

Fig. 2a shows XRD typical results of TMCs oxidized at 823, 873, 923 K for 300 h. It is found that the reaction products are predominantly rutile TiO_2 and α-Al_2O_3. In order to further analyse the formation of the oxide phases of TMCs, the Ti 2p and Al 2p XPS spectras recorded the surface subsequent to oxidation within 300 h are shown in Fig. 2b. It is clear that the Al 2p spectra and Ti 2p spectra are the Al_2O_3 and TiO_2, respectively. The other oxide B_2O_3 was not detected by XPS and XRD.

Typical features of the outer surfaces of the specimens after oxidation are shown in Fig. 3. It is evident that the oxide scale and the oxide morphology here formed on Ti-Al are different than that formed on TMCs at the same oxidation temperature, as depicted in Fig. 3a and b. As distinct from Ti-Al, the size of oxide formed on TMCs is finer (Fig. 3a and b). The size

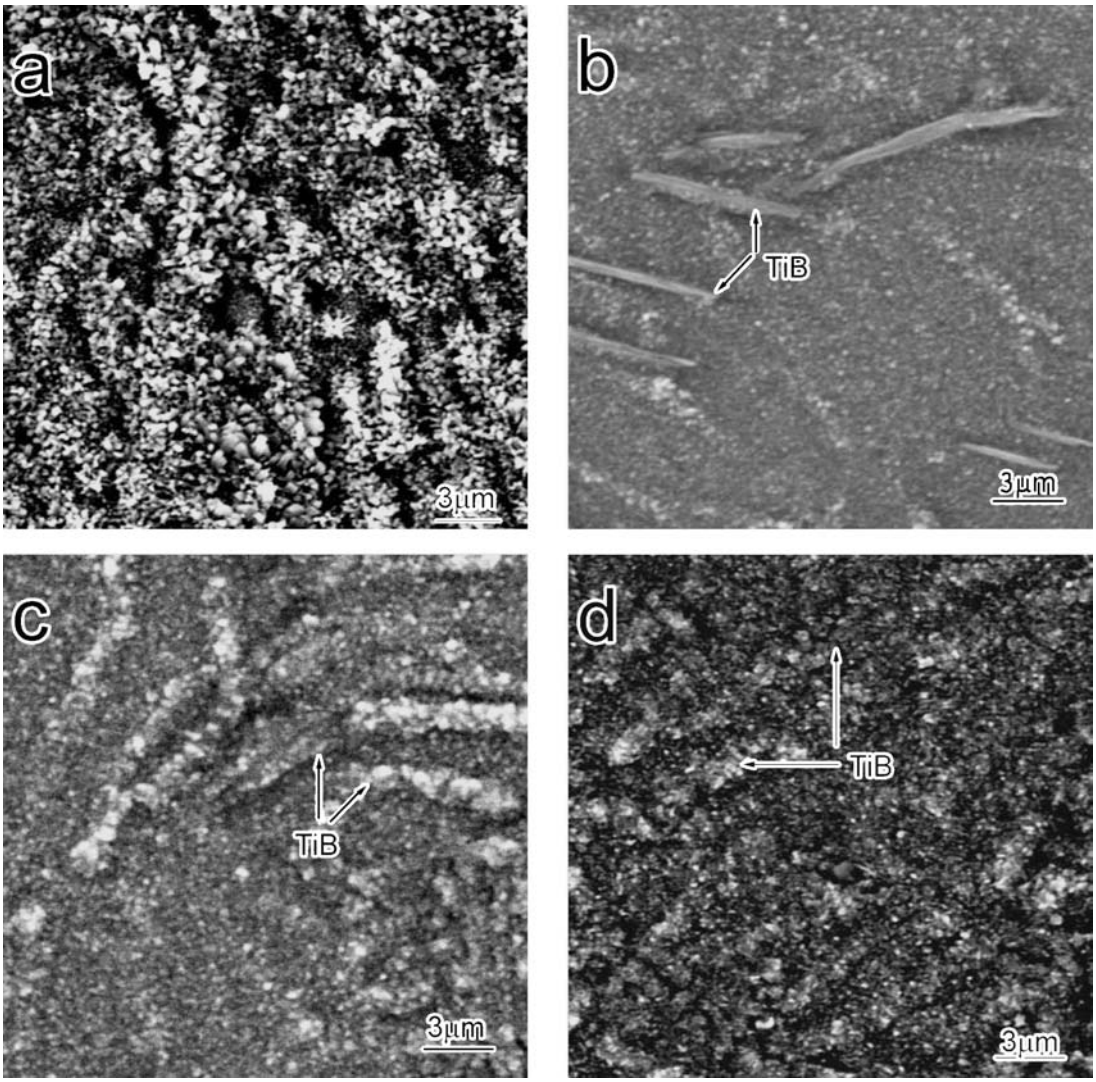

Figure 3 SEM micrographs (Secondary Electron Micrographs) of surface oxides of (a) Ti-Al at 823 K, (b) TMCs at 823 K, (c) TMCs at 873 K, and (d) TMCs at 923 K for 300 h.

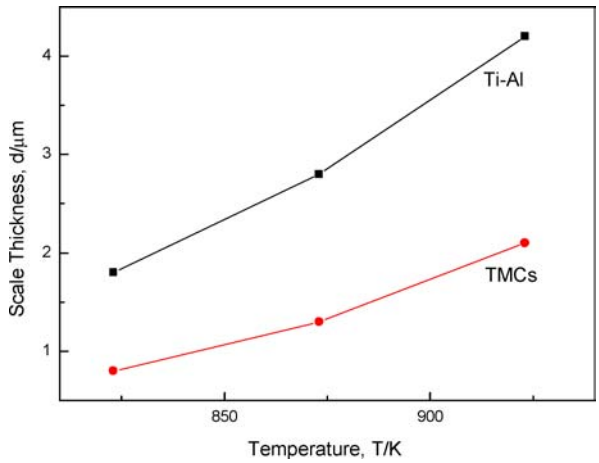

Figure 4 Measured average scale thickness of TMCs and Ti-Al after oxidation at 823, 873, and 923 K for 300 h.

of oxide crystal for oxidation of TMCs increases with the increase of temperature. Moreover, the top scale formed on TMCs is continuous and free from cracks Fig. 3b–d). It is of great importance for a practical engineering material used at elevated temperatures.

Generally speaking, TiB oxidizes according to the following chemical reaction,

$$\frac{4}{7}\mathrm{TiB}(s) + \mathrm{O}_2(g) \rightarrow \frac{4}{7}\mathrm{TiO}_2(s) + \frac{2}{7}\mathrm{B}_2\mathrm{O}_3$$

(solid if $T < 723$ K and liquid if $T > 723$ K) [9]

Since the mass-change curves of TiB/Ti-Al composites can be affected by weight loss for B_2O_3 vaporization, as well as weight gain for scaling [10], the thickness of each oxide scale was measured and is displayed in Fig. 4. Four measurements were taken to arrive at each average value, and the standard deviations are all within 5%. Fig. 5 reveals the microstructure of a cross section of the oxide scale on TMCs and Ti-Al after isothermal oxidation at 923 K for 300 h. For TMCs, the oxide scale is very thin, only about 2 μm (Fig. 5a). Oxide scale of Ti-Al is shown in Fig. 5c, it is thicker (more than 4 μm) than that of TMCs. In accordance with Figs 4 and 5, the addition of TiB can decrease the thickness of oxidation, so the addition of reinforcements can improve the oxidation resistance of TMCs.

In an attempt to understand what is occurring at the reinforcements, typical features of the TiB after oxidation are shown in Fig. 6a and d. Basically, TiB particles generally maintained their original rod-shape, although they were oxidized partly and the oxide scale consists of a large number of very small grains in the order of 2 nm. The SAD patterns around spot 1, which are diffraction rings shown in Fig. 6b, can be indexed with reflection of TiO_2 (rutile). The analysis of the diffraction pattern around spot 2 yields reflection of α-Al_2O_3 (Fig. 6c). It can be seen from TEM images (Fig. 6d) that the interface between TiB and the titanium matrix alloy after oxidation is still clean, flat and sharp. There is no interfacial reaction and any changes in the interface. The examination of the TiB-oxide interface shows that apart from rutile TiO_2, nitrides or other oxides were not identified by selection electron diffraction and EDX analyses. The EDX results which were obtained by spot analysis only show peaks of titanium and oxygen at the TiB-oxide interface. It is well known that TiB oxidizes to TiO_2 and B_2O_3. It was reported that B_2O_3 evaporates considerably at 1073 K [9]. The above results then show that the TiB partially transformed into amorphous boron oxide after oxidation in the present test temperature.

The results of isothermal oxidation show that the addition of the reinforcements can improve the oxidation resistance of the TMCs. The reason for the encouraging result in the present study can be addressed for this improvement.

Oxide scales formed on the composites were composed mainly of very small oxide grains. It is related to the microstructure of the *in situ* synthesized TMCs. As discussed in the former papers [3–6], *in situ* synthesized reinforcements TiB are uniformly distributed in the titanium matrix alloy. These uniformly distributed *in situ* synthesized TiB particles can act as heterogeneous nucleation sites for oxidation by providing high surface areas to oxygen and reduce the internuclear

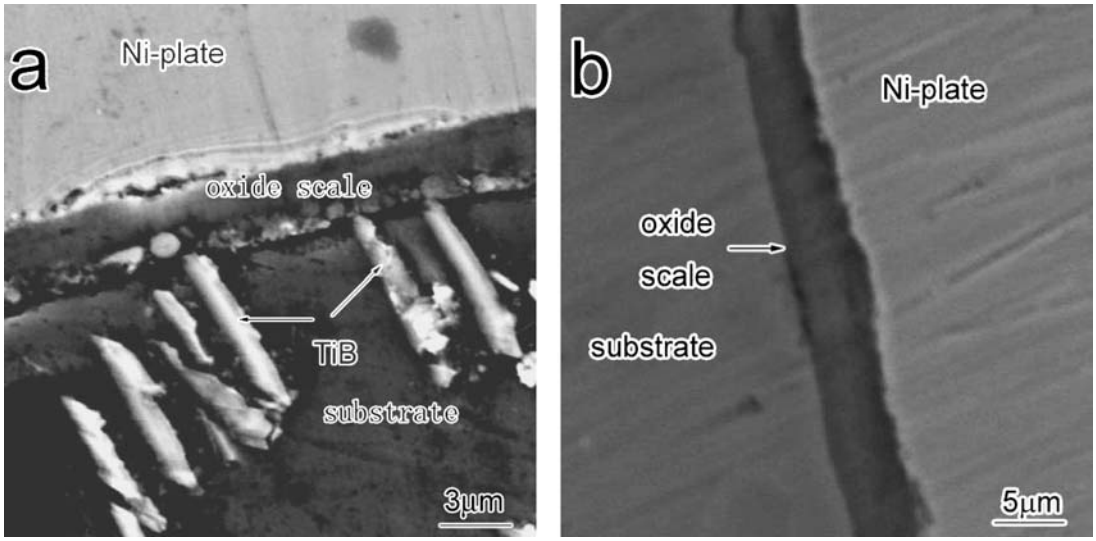

Figure 5 SEM micrographs (Secondary Electron Micrographs) of oxides on the cross-section of (a) TMCs and (b) Ti-Al after oxidation at 923 K for 300 h.

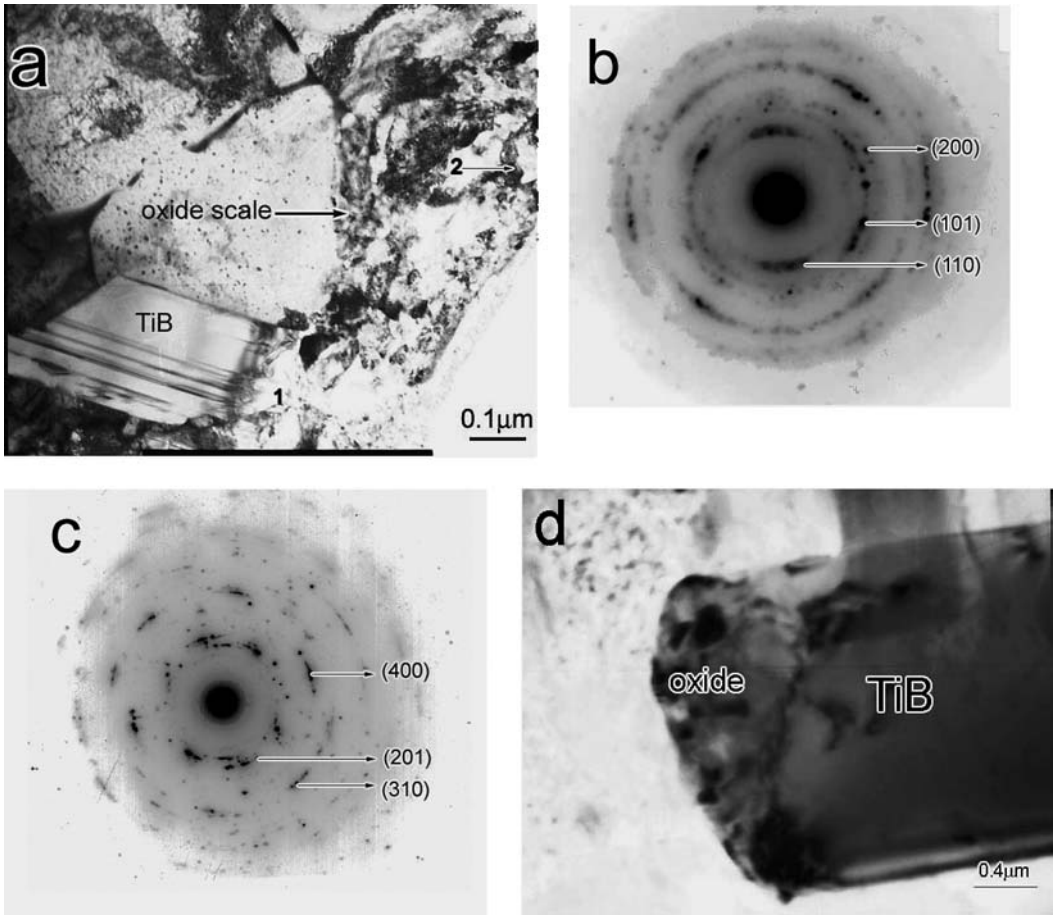

Figure 6 TEM results of TMCs (a) cross-section image around the TiB fiber; (b) SAD pattern around 1 (TiO_2), (c) SAD pattern around 2 (α-Al_2O_3), and (d) bright field TEM image of TiB/Ti-Al interface after oxidation at 923 K for 300 h.

distance. Moreover, the reinforcements can decrease the size of the matrix alloy. Also, the high density of grain boundaries could significantly accelerate the oxidation stage, and then shorten the distance between the nuclei. All these factors fine the oxide grains. Plastic deformation and creep of the scale are favored by small grain size [11, 12]. Therefore, the growth and thermal stresses could be effectively released through scale deformation, avoiding cracking and spallation. And, in the early stages of *in situ* synthesized TMCs during fabrication, nuclei of these uniformly distributed TiB particles are formed. These nuclei form by depleting the surrounding region of titanium. This causes an enrichment of other element and favors the formation of its oxide during oxidation. Hence, this caused the enhanced alumina-forming tendency of TMCs.

As the size of grain in the substrate is rather small, preferential oxidation in grains or along grain boundaries and phase interfaces could take place on microdimensions, resulting in rugged and rough interface on the composite samples. Some parts of the scale penetrated into the substrate, penning itself firmly to the matrix and keeping the integrity of the interface.

The coefficients of thermal expansion (CTE) of Ti, TiB, and TiO_2 are 8.2×10^{-6}/K, 8.6×10^{-6}/K, and 7.0–8.7×10^{-6}/K, respectively [13]. The CTEs of the scale and substrate are closer with TiB and TiC reinforcements, which will lower thermal stress. Lower thermal stress reduces the tendency of scale cracking and spallation.

All above show that the oxide scales formed on TMCs are dense and have good adherence to the substrate. Furthermore, TEM results reveal that the interface cohesion between the reinforcements and the titanium matrix alloy is strong enough and the interfacial microstructure of TiB/Ti-Al before and after oxidation is clean. Consequently, *in situ* synthesized TiB reinforcements can slow down the oxidation rate of the composites.

4. Conclusions

(1) The activation energy for oxidation of TiB/(Ti-Al) is 297.6 KJ/mol and that of Ti-Al is 225.8 KJ/mol.

(2) The oxidation kinetics of *in situ* synthesized TiB/Ti-Al composites at temperatures between 823 and 923 K in air for 300 h basically follow a parabolic rate law.

(3) The oxidized surface of both the composite and the alloy consists of a mixture of rutile-TiO_2 and α-Al_2O_3, and TiB partially transformed into amorphous boron oxide.

(4) The reinforcements TiB can improve the oxidation resistance due to uniform distribution of *in situ* synthesized reinforcements and finer microstructure, which make oxide grain refinement, thin and dense. The enough strong interface cohesion and the clean

interfacial microstructure between the reinforcements and the titanium matrix alloy before and after oxidation can contribute to the improvement of oxidation resistance of the composite.

Acknowledgments

We would like to acknowledge a financial support provided by A Foundation for the Author of National Excellent Doctoral Dissertation of P R China under Grant No: 200332, Research Fund of Science and Technology Commission of Shanghai Municipality under Grant No: 04DZ14002, 04QMX1412 and ItoYama Foundation.

References

1. D. B. LEE, M. H. KIM, C. M. YANG, C. H. LEE and M. H. YANG, *Oxid. Met.* **56** (2001) 215.
2. G. Z. LUO, *Rare Met. Mater. Eng.* **26** (1997) 1 (in Chinese).
3. X. N. ZHANG, W. J. LU, D. ZHANG, R. J. WU, Y. J. BIAN and P. W. FANG, *Scripta Metall. Mater.* **41** (1999) 39.
4. W. J. LU, D. ZHANG, X. N. ZHANG, R. J. WU, T. K. SAKATA and H. MORI, *Mater. Trans. JIM* **41** (2000) 1555.
5. Y. X. QIN, W. J. LU, X. F. SHENG, Z. F. YANG and D. ZHANG, *ibid.* **44** (2003) 2282.
6. W. J. LU, D. ZHANG, X. N. ZHANG, Y. J. BIAN, R. J. WU, T. SAKATA and H. MORI, *J. Mater. Sci.* **36** (2001) 3707.
7. B. G. VELASCO and P. B. ASWATH, *ibid.* **33** (1998) 2203.
8. J. D. MAJUMDAR, B. L. MORDIKE, S. K. ROY and I. MANNA, *Oxid. Met.* **57**(5/6) (2002) 473.
9. D. B. LEE, Y. C. LEE and D. J. KIM, *ibid.* **56** (2001) 177.
10. A. BELLOSI, T. GRAZIANI, S. GUICCIARDI and A. TAMPIERI, in Proceedings of the 9th Special Ceramics Conference, London, December 1990 (British Ceramics Society, London, 1992).
11. S. A. KEKARE, J. B. TONEY and P. B. ASWATH, *Metall. Mater. Trans. A* **26** (1995) 1835.
12. B. G. VELASCO and P. B. ASWATH, *J. Mater. Sci.* **33** (1998) 2203.
13. A. P. MAJID and C. ZWEBEN, "Comprehensive Composite Materials, col. 1" edited by A. Kelly (Elsevier, Amsterdam, 2000).

Received 4 November 2004
and accepted 26 April 2005